Divertor Simulation Study Using the GAMMA 10 End-Mirror Cell*)

Hisato TAKEDA, Yousuke NAKASHIMA, Katsuhiro HOSOI, Kazuya ICHIMURA, Tetsuro FURUTA[1)], Kazuhiko HIGASHIYAMA[1)], Mitunori TOMA[1)], Akiyoshi HATAYAMA[1)], Takashi ISHII, Hideaki UEDA, Mizuki SAKAMOTO, Makoto ICHIMURA, Masayuki YOSHIKAWA, Junko KOHAGURA and Tsuyoshi IMAI

Plasma Research Center, University of Tsukuba, Tsukuba, Ibaraki 305-8577, Japan
[1)]*Science and Technology, Keio University, Hiyoshi, Yokohama 223-8522, Japan*

(Received 11 December 2011 / Accepted 3 August 2012)

In GAMMA 10 which is a tandem mirror machine in Plasma Research Center at University of Tsukuba, divertor simulation studies have been planned and started. This paper describes the recent results of divertor simulation experiment in the GAMMA 10 end-mirror cell. As a part of these experiments, characteristics of end-loss plasma have been investigated by using probes and calorimeters. The diagnostics are installed at two positions, which are separated by 40 cm in the axial direction. In the results, ion temperature of the end-loss flux in GAMMA 10 is much higher than that of other divertor simulators. It is found that heat-flux density can be controlled within the range from 0.4 to 0.8 MW/m^2 by changing the ICRF power. In addition, heat flux density has strong dependence on diamagnetism in the central-cell which is time integrated in the plasma duration. While, particle-flux density is proportional to electron line-density in the central-cell. Particle and heat fluxes measured at axially different positions agree well with the calculation results for considering the influence of particle reflection phenomena.

Keywords: divertor simulation, GAMMA 10, tandem mirror, probe, calorimeter, heat flux, particle flux

DOI: 10.1585/pfr.7.2405151

1. Introduction

In the International Thermonuclear Experiment Reactor (ITER) and Demo reactor for future nuclear fusion power generation, heat load of plasma particles led to divertor plates approaches 10~20 MW/m^2 on steady-state operation. In addition, it reaches 0.5~1.0 GW/m^2 when ELM occurs. Therefore, it is important to develop divertor plates which attain the level of high heat-load from the divertor plasma. For solving this problem, it is needed to find out the physical mechanism to keep the divertor plates detached from the plasma influx steadily [1–3]. For studying divertor physics, it is useful to simulate plasma in SOL and divertor regions in actual fusion devices by the liner devices. Thus, the divertor simulation experiments are widely performed by using liner device [4–6].

GAMMA 10 which is a tandem mirror machine in Plasma Research Center at Tsukuba University is the world's largest liner device. In GAMMA 10, divertor simulation experiments were planed and started by introducing new divertor systems to existing tandem mirror device for contribution to the toroidal plasma research [7, 8]. These new two divertor systems are called A-Divertor and E-Divertor. A-Divertor is designed for the development of new divertor containing a separarix configuration. While, E-Divertor is a high-heat flux divertor simulator by use of end-cell of the large tandem mirror device. By using these devices, we approach research subjects of the boundary plasma.

In this paper, experimental results about E-Div. are discussed. In section 2, experimental set up about E-Div. is described and experimental results are shown in section 3. The summary is presented in section 4.

2. Experimental Set Up

Figure 1 shows the schematic view of GAMMA 10. GAMMA 10 consists of a central-cell, two anchor-cells, two plug/barrier-cells and two end-cells. Plasma is generated mainly in the central-cell. Anchor-cells are equipped for MHD stability by minimum-B magnetic configuration. High electro-static potential can be formed by injecting ECH in plug/barrier-cell. The end-cells are located at both ends of GAMMA 10. In this region, end-loss particles which are not confined by five magnetic mirrors are transported toward both ends. Therefore, E-Div. experiments are performed at the west end-cell in GAMMA 10. This region is shown in Fig. 2.

High power plasma heating systems which are com-

author's e-mail: takeda_hisato@prc.tsukuba.ac.jp
*) This article is based on the presentation at the 21st International Toki Conference (ITC21).

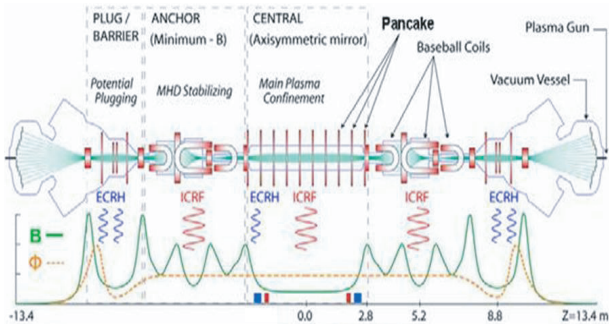

Fig. 1 The schematic view of GAMMA 10.

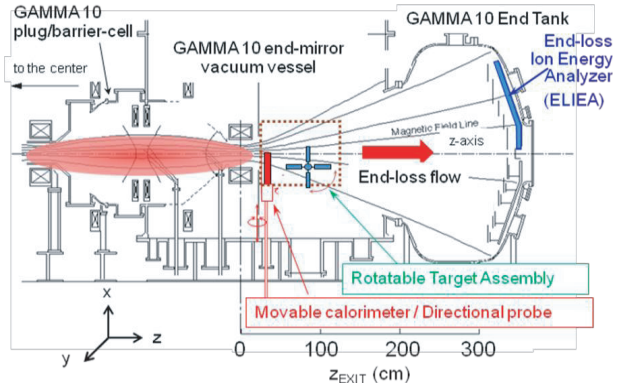

Fig. 2 The schematic view of the experimental set up in the GAMMA 10 west end-cell.

posed of ion cyclotron range of frequencies (ICRF) waves, neutral beam injection (NBI) and electron cyclotron heating (ECH) are installed for plasma production, heating and confinement. By applying ICRF in the central-cell and anchor-cells, end-loss ion can be generated with much higher ion temperature than electron temperature. In this plasma state, contribution of ion dominates the heat-flux density. In case of superimposing ECH in plug/barrier-cells on ICRF-produced plasma, on the other hand, the contribution of electron becomes significant.

In this E-Div. experiments, as shown in Fig. 2, we have installed a set of directional probe and movable calorimeters which are made of copper and rotation target near the exit of the end-mirror coil in the west end-cell (z_{EXIT} = 30, 70 cm). By using these diagnostics, axial and radial profiles of particle-flux and heat-flux of end-loss plasma have been measured precisely.

3. Experimental Results and Discussion

In typical hot-ion-mode plasma ($n_e(0) = 2\times10^{18}$ m^{-3}, $T_i(0) = 5$ keV), measurement of heat and particle flux from the end-mirror exit was performed as shown in Fig. 2. Heating systems used in this experiment were ICRF1, 2 and 3. ICRF1 is equipped for plasma generation and stabilization by heating ions in the anchor-cells. ICRF2 is

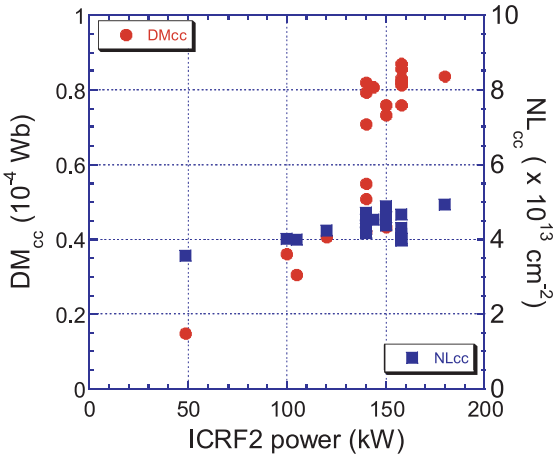

Fig. 3 ICRF2 power dependence on diamagnetism and electron line-density. The circle plots show diamagnetism in the central-cell and the square plots show electron line-density in the central-cell.

used for ion heating in the central-cell. ICRF3 is used for increasing plasma density in the anchor-cell.

3.1 Heating power dependence of heat and particle fluxes

As previously explained, main plasma in GAMMA 10 is produced at the central-cell and then leeks toward both end-cells through coulomb collision which is a dominant factor for the production of end-loss ions. Therefore, it is important to investigate the relationship between main plasma parameter of the central-cell and heat and particle fluxes at the end-cell.

In order to achieve higher heat-flux, the plasma parameter dependence in plasma heating power has been investigated. Figure 3 shows the temporal behavior of the main plasma parameters in the central-cell at different ICRF powers. The diamagnetism in the central-cell increases with ICRF power. On the other hand, the electron line-density in the central-cell keeps almost constant on the ICRF power.

Figure 4 shows the ICRF2 power dependence on heat and particle fluxes. In this experiment, the gas-puffing rate was almost kept constant. These data are obtained from the similar condition except for ICRF2 power. Heat flux has been measured by measuring the temperature change of the calorimeter during one plasma shot. In addition, obtained values are measured on the axis of the GAMMA 10. From Fig. 4, the heat flux is clearly observed to be proportional to ICRF2 power. On the other hand, particle flux dependence on ICRF2 power is weaker than the heat flux. It is seemed that the plasma confinement in mirror field is improved by increasing ICRF2 power because ion collision time becomes long for higher ion temperature. This fact does not explain results of Figs. 3, 4 completely. For example, excited wave which is generated by anisotropy of

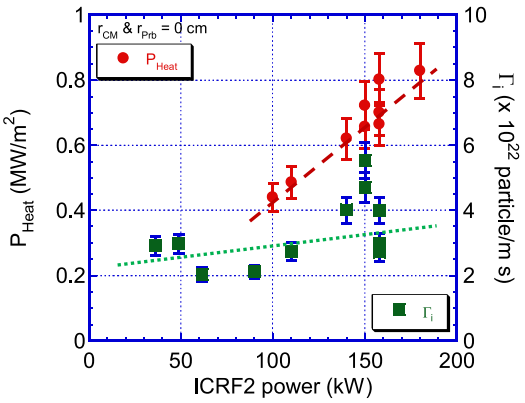

Fig. 4 ICRF2 power dependence on heat and particle fluxes. Circle symbols show heat flux and square symbols show particle flux.

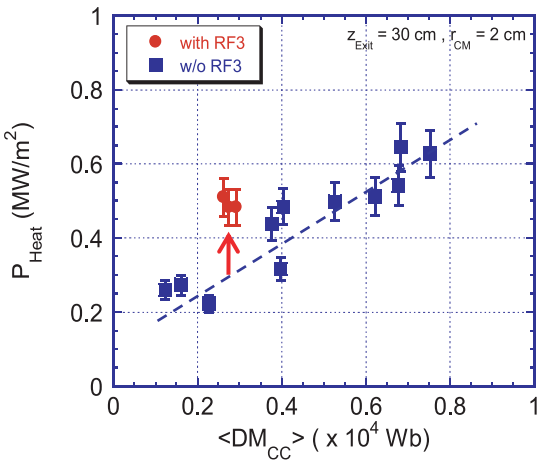

Fig. 5 Heat flux dependence on the time integral diamagnetism in the central-cell.

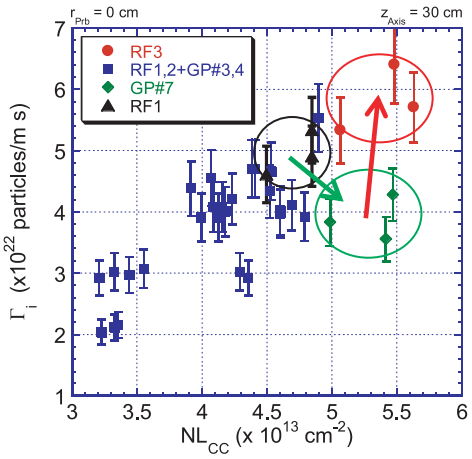

Fig. 6 Particle flux dependence on electron line-density in the central-cell. NL_{CC} were changed by using plasma heating and gas puff systems.

ion temperature may drive ions toward the end-cell.

From these results, ICRF heating affects heat and particle fluxes, which suggest that heat and particle flux can be increased more by additional ICRF plasma heating.

3.2 Additional heating effects at heat and particle fluxes

ICRF in the central-cell (each ICRF1 and 2) is limited to maximum power of 180 kW. Additional heating effects on heat and particle fluxes have been investigated by applying ICRF power into not the central-cell but the anchor-cell.

In order to enhance MHD stability, additional ICRF plasma heating systems was installed in the east anchor-cell. This plasma heating system is called ICRF3. By superimposing ICRF3 in the east anchor-cell, the electron line-density in the central-cell and the east anchor-cell increased in spite of decreasing the diamagnetism in the central-cell. Ion flux measured by multi-gridded type energy analyzer also increases drastically at the west end-cell [9].

By using this additional heating system (ICRF3), relationship between heat/particle fluxes and main plasma parameters in the central-cell was investigated. In the case of heat flux, the results measured at radially 2 cm from the axis are shown in Fig. 5. In the experiment, quantity of gas puff and the power of ICRF1 and 2 are changed to control the diamagnetism in the central-cell. The heat flux has a linear relationship with the time integral diamagnetism <DMcc>. From the figure, heat flux increased about 70 percent in the case of superimposing ICRF3. Therefore, the heat flux on the axis is expected to increase similarly. Basically ICRF3 does not contribute to increase diamagnetism in the central-cell directly. However, the electron line-density and diamagnetism in the anchor-cell is confirmed to be increased by applying ICRF3. As the result, the heat flux seems to be increased at the end-cell.

The result of particle flux measurement is shown in Fig. 6. The quantity of gas puffing was changed for increasing plasma density in the central-cell. The particle flux is almost proportional to electron line-density in the central-cell (NL_{CC}). In the case of using only ICRF1, 2 and gas puff in the mirror throat of the central-cell (GP#3, 4), the particle flux increases up to 5.5×10^{22} particle/m^2·s. By adding gas puff in the central-cell mid-plane (GP#7), however, the particle flux decreases in spite of increasing NLcc. In case of gas puff (#7), it is found that the fluctuation of line-density and diamagnetism is observed, which indicates radial particle loss due to MHD instability. It is expected that these degradation of plasma performance can be improved by anchor heating with ICRF3. By superimposing ICRF3, the particle flux is stably increased up to 6.5×10^{22} particle/m^2·s.

The results of Figs .5 and 6 suggest that additional plasma heating in the end-mirror region can continue to increase the particle and heat-flux density, which gives a clear prospect for achieving higher particle and heat fluxes

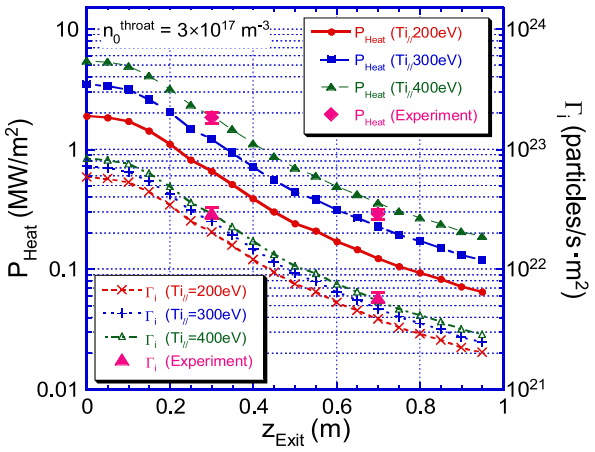

Fig. 7 Axial profile of heat and particle flux. Calculation results are shown as solid and broken line.

suitable for divertor simulation studies.

3.3 Effects of particle reflection

In this section, the influence of reflection particle in measuring heat flux by using calorimeter was considered. In the previous study, radial profile of heat and particle fluxes was measured at different axial positions. Each profile normalized at the central-cell mid-plane position according to the shape of the magnetic flux tube showed a good agreement at different axial positions [10]. Therefore, it was confirmed that the transport of the heat and particle fluxes from the end-mirror exit was basically governed by the magnetic field configuration in the end-mirror region. For investigating the above result in detail, an axial distribution of heat and particle fluxes is compared with the calculation. Here, propagation and expansion of end-loss ions along the magnetic field are calculated by giving initial values of density and temperature of the mirror throat. The result is shown in Fig. 7

In this calculation, the ion density was assumed to be $n_0 = 3 \times 10^{17}\,\mathrm{m}^{-3}$ at the end-mirror exit. The parameters of $T_{i//}$ were also assumed to be 200 eV, 300 eV and 400 eV. Experimental value of the heat flux is corrected by the effect of particle reflection as follows [11]. Relationship between the measurement and the corrected value of the particle energy E is shown as,

$$E = E^{\mathrm{measure}}/[1 - (R_E/R_x)], \quad (1)$$

where E^{measure} is the energy determined from measured results of calorimeter and probes. R_E and R_N are energy reflection coefficient and particle reflection coefficient, respectively. The values of R_N, R_E are determined from the data base in Ref. [11]. The R_E/R_N value is estimated to be 0.62 based on the experimental data. By considering the influence of particle reflection, it was estimated that $T_{i//}$ (temperature of parallel to the line magnetic force) was about 400 eV from the calculation. From Fig. 7, good agreement is observed between calculation and experimental values. This value has been also confirmed by multi-gridded type energy analyzer (ELIEA).

4. Summary

Divertor simulation study has been started in PRC, University of Tsukuba by introducing new divertor system (E-Div.). The characteristics of end-loss ion flux were investigated based on the experimental data obtained with probe and calorimeter.

1. Heat and particle flux significantly depends on diamagnetism and electron line-density in the central-cell respectively
2. Experimental result of superimposing ICRF3 in the east anchor-cell suggests that additional plasma heating in end-mirror region can contribute to increase of the heat and particle flux
3. By considering the influence of particle reflection, $T_{i//}$ in the end-cell is estimated to be about 400 eV in this experiment and its axial profile agree well with the calculation results.

Acknowledgement

This work is supported by the bidirectional collaboration research program in the university of Tsukuba (NIFS09KUGM037). The authors would like to thank the members of the GAMMA 10 groups for their collaboration in the experiments and for helpful discussion.

[1] E. Tsitrone, J. Nucl. Mater. **363-365**, 12 (2007).
[2] A.S. Kukushkin *et al.*, Nucl. Fusion **42**, 187 (2002).
[3] A. Loarte *et al.*, J. Nucl. Mater. **266-269**, 118 (1999).
[4] Y. Hirooka *et al.*, J. Vac. Sci. Technol. A**8**, 1790 (1990).
[5] S. Masuzaki *et al.*, Jpn. J. Appl. Phys. **29**, 2835 (1990).
[6] B. Koch *et al.*, J. Nucl. Mater. **290-293**, 653 (2001).
[7] Y. Nakashima *et al.*, Fusion Eng. Des. **85**, Issue 6, 956 (2010).
[8] Y. Nakashima *et al.*, 23rd IAEA Fusion Energy Conference (October 11-16, 2010, Daejeon, Korea) IAEA-CN-180FTP/P1-33.
[9] K. Ichimura *et al.*, in the same proceeding.
[10] Y. Nakashima *et al.*, Trans. Fusion Sci. Technol. **59**. No.1T, 61 (2011).
[11] R. Behrisch and W. Eckstein, *Physics of Plasma-Wall Interactions in Controlled Fusion*, ed. by D.E. Post and R. Behrish, NATO ASI Series B: Physics Vol.131 (Plenum Press, New York, 1986).